



ELSEVIER

Signal Processing III (IIII) III-III

SIGNAL  
PROCESSING

www.elsevier.com/locate/sigpro

1  
3  
A HMM approach to the estimation of random trajectories  
on manifolds ☆

Jorge S. Marques<sup>a,b,\*</sup>, João M. Lemos<sup>a,c</sup>, Arnaldo J. Abrantes<sup>d</sup>

<sup>a</sup>Instituto de Sistemas e Robotica, Av. Rovisco Pais, 1049-001 Lisbon, Portugal

<sup>b</sup>Instituto Superior Técnico, Av. Rovisco Pais, 1049-001 Lisbon, Portugal

<sup>c</sup>INSEC, Portugal

<sup>d</sup>ISEL, Portugal

Received 9 June 2000

5  
7  
9  
**Abstract**

11 Dynamic image analysis requires the estimation of time-varying model parameters (e.g., shape coefficients). This can be  
13 seen as states of a dynamic model which are restricted to a subset of Euclidean space. This paper describes an algorithm  
15 for the estimation of the state evolution on manifolds exploiting three sources of information: the manifold geometry, the  
motion model and the sensor model. Examples are provided to illustrate the performance of this method in situations where  
classic procedures cannot perform well. © 2002 Published by Elsevier Science B.V.

*Keywords:* Image analysis; Object tracking; Hidden Markov models; Manifold estimation

11  
13  
15  
**1. Introduction**

19 Dynamic image analysis requires the estimation  
21 of time-varying model parameters (e.g., shape co-  
23 efficients). This can be seen as states of a dynamic  
model which are restricted to a subset of Euclidean  
space. Typical examples are the estimation of objects  
motions (e.g., cars) or the evolution of objects shapes  
(e.g., mouth contour, heart cavities) from video se-  
quences. Hereafter, state is to be understood in this

25 way. A common factor present in most estimation  
27 problems is the fact that unknown variables exist in  
29 high-dimensional spaces but they cannot take arbitrary  
31 values. Instead, they are usually restricted to smooth  
33 subsets (e.g., surfaces) (Fig. 1). These subsets often  
35 have a complex structure and must be estimated from  
37 the observation data. The following examples illus-  
39 trate this point. Consider the problem of visual track-  
41 ing of cars in a lane. A simple prototype situation is  
considered below in this paper. Since the lane geom-  
etry will enforce the trajectory, this is a valuable in-  
formation for reducing the computational load of the  
search algorithm and furthermore enhances the robust-  
ness of the position estimation. Classical algorithms  
i.e., which do not restrict the state variables to a man-  
ifold, are more prone to yield instabilities in the track-  
ing error. This drawback is even more serious when  
the observations of the car position are drawn from

☆ This work was partially supported by PRAXIS XXI under project EEI/12050/1998 (Tracking of Moving Objects).

\* Corresponding author. Instituto de Sistemas e Robotica, Instituto Superior Técnico, Torre Norte, AV. Rovisco Pais, 1049-001 Lisbon, Portugal. Tel.: +351-1-310-0000; fax: +351-1-314-5843.

E-mail addresses: jsm@isr.ist.utl.pt (J.S. Marques), jlml@inesc.pt (J.M. Lemos), aja@cedet.isel.pt (A.J. Abrantes).

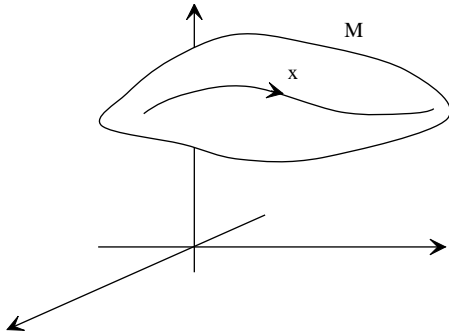


Fig. 1. Trajectory on a manifold.

omnidirectional sensors which measure only the distance to the target. An example is given below. Where these examples refer to the actual position of the moving object constrained to a manifold, one can also think of its motion parameters also being constrained. For instance, let the car velocity be modeled as the low-pass filtering of white noise with a given bandwidth (BW). If BW slowly varies in time, being constrained to some subset of values, the methods to be considered in this paper may also be applied with advantage.

In static problems (e.g., in image reconstruction and object recognition) attempts have been made for incorporating known restrictions in the estimation process [6,11,13]. Two types of constraints are usually considered: hard constraints which lead to the use of constrained optimization methods (e.g., POCS [1,7]) or soft constraints based on the use of regularization techniques or prior information [12]. In [6] three-dimensional object views are represented as a linear combination of eigen images multiplied by appropriate coefficients. Although the number of coefficients is very high, the number of degrees of freedom is much smaller i.e., when the view changes the coefficients describe a trajectory on a low dimension manifold. Advantage is taken of this fact for object recognition.

In dynamic scene analysis, state constraints play an even more important role for two main reasons: (i) they significantly improve the trajectory estimates (the improvement being often dramatic, e.g., a nonobservable system may become observable if appropriate restrictions are used) and (ii) they allow one to formulate the estimation problem in a lower dimension subspace (the dimension of the working subspace depends on the manifold dimension and not on the data dimen-

sion). Both effects are instrumental for achieving good results and should be considered in the design of trajectory estimation algorithms [3,2]. In [3] geometric restrictions are used for lip tracking. Although lips are represented by 40 control points belonging to a space of dimension 80, by exploiting the constraints in the control point movement, estimation has only to be performed in a space of dimension 5. Other examples are provided by in the analysis of Human gestures. In [2] gestures are described by a one-dimensional manifold denoted as *principal curve*.

In this paper, by considering a general framework for trajectory estimation on manifolds, a specific algorithm to solve this problem under a general hypothesis is proposed. By relying on discrete approximation and hidden Markov model (HMM) techniques, an algorithm for trajectory estimation on manifolds is derived. Illustrative examples are presented.

## 2. Estimation framework

The problem is stated as follows: Let  $x$  be an unknown trajectory defined in a manifold  $\mathcal{M} \subset \mathbb{R}^n$ . The trajectory  $x$  is to be retrieved from a sequence of nonlinear and noisy observations  $y$ . It will be assumed that  $x$  is a realization of a stochastic process defined on the manifold and  $y$  consists of nonlinear and noisy observations of  $x$  values; these processes are characterized by a motion model  $p(x_t/x_{t-1})$  and by a sensor model  $p(y_t/x_t)$  that have to be estimated from the data.

The overall solution to this problem involves three steps: (i) manifold learning; (ii) motion and sensor model learning; and (iii) trajectory retrieval. The first steps are performed off line while the last step is performed on line. It will be assumed that a set of  $(x, y)$  sequences is known forming a training set employed in steps (i) and (ii).

In the first step the manifold is estimated from known  $x$  trajectories (Fig. 2). The manifold is segmented into a set of regions and each region is described by a parametric function defined on a local coordinate system: a hyperplane is fitted to each region defining a low dimension subspace of independent variables; the projection error is not neglected, being modeled as a dependent variable.

In the second step, two models, a motion model and a sensor model, are estimated from the data. The

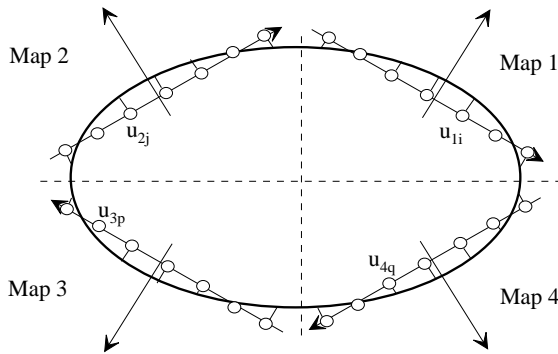


Fig. 2. Manifold model.

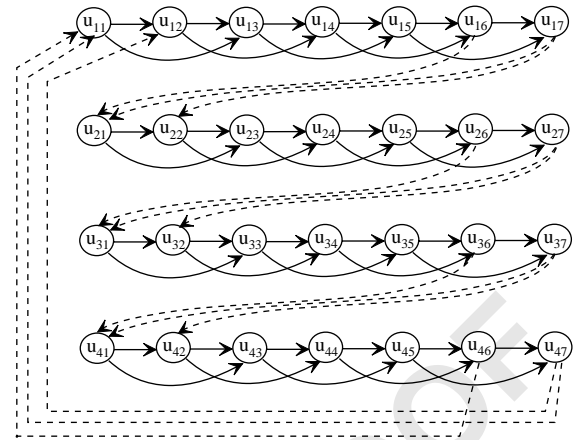


Fig. 3. Motion model: local and global Markov models.

1 motion model defines the allowed transitions between  
 3 points in the manifold and the corresponding probabili-  
 5 ty associated with the transitions. Three approaches  
 7 can be considered for describing the motion of a point  
 9 on the manifold: a continuous time approach, a dis-  
 11 crete time approach with continuous state and a dis-  
 13 crete approach based on time and state discretization.  
 15 The first approach requires the use of a stochastic dif-  
 17 ferential equation defined on the manifold. This topic  
 19 has been addressed in the controls literature [4,5] and  
 21 can be pursued in the context of trajectory estima-  
 23 tion. The second approach leads to the use of differ-  
 25 ence equations. The third approach is based on dis-  
 27 crete time and discrete state models, discrete Markov  
 29 models being an appealing solution.

A sensor model defining the probability distribu-  
 17 tion of the observed data for each manifold point is  
 19 also needed and has to be estimated from the data.  
 21 The previous steps concern manifold learning and  
 23 motion/sensor learning. The third step is the estima-  
 25 tion of trajectories on the manifold assuming that the  
 27 manifold and the motion/sensor models are known.  
 29 The solution of this problem depends on the models  
 31 considered. The continuous time approach is based on  
 33 stochastic differential equations, leading to the use of  
 nonlinear observers on manifolds and will not be pur-  
 sued here. A second approach based on the discrete  
 state formulation is adopted in this paper, leading to  
 a set of HMMs (a model per manifold region) linked  
 by transitions among different regions.

In the example considered in Fig. 2 it is assumed  
 that a point moves clockwise with a limited velocity.  
 This results in a Markov chain with transitions to one  
 of two consecutive states (see Fig. 3). This is just an

example of a Markov chain which can arise in such  
 a type of problems. Other structures of the Markov  
 chain modeling motion may be considered.

### 3. The discrete manifold analysis (DMA) algorithm

This section describes an algorithm for the es-  
 timation of trajectories on manifolds. This algo-  
 rithm, denoted as DMA, provides a solution for the  
 three problems described before: manifold learning;  
 motion/sensor model learning and trajectory retrieval.

#### 3.1. Manifold learning

The DMA algorithm splits the manifold into  $M$  re-  
 gions and approximates each region by a set of cen-  
 troids (Fig. 2). Centroid computation is performed in  
 a low dimension hyperplane estimated from the data.

Let  $X$  be a set of manifold points (training set). It  
 will be assumed that the elements of  $X$  are realiza-  
 tions of a random variable whose distribution is ap-  
 proximated by a mixture of Gaussians

$$p(x) = \sum_{k=1}^M c_k N(x; \mu_k, R_k), \quad (1)$$

where  $M$  is the number of modes and  $N(x; \mu, R)$   
 denotes a normal density function with mean  $\mu$   
 and covariance matrix  $R$ . Under this hypothesis the  
 expectation-maximization method (EM) is used to

1 estimate the means  $\mu_i$  and covariances  $R_i$  of the  
2 Gaussian modes [9] according to

3 *Fuzzy classification (E-step):*

$$\pi_k(x) = \frac{\hat{c}_k N(x; \hat{\mu}_k, \hat{R}_k)}{\sum_{i=1}^M \hat{c}_i N(x; \hat{\mu}_i, \hat{R}_i)}. \quad (2)$$

*Update (M-step):*

$$\hat{c}_k = \frac{1}{\#X} \sum_{x \in X} \pi_k(x), \quad (3)$$

$$\hat{\mu}_k = \frac{1}{\#X \hat{c}_k} \sum_{x \in X} \pi_k(x) x, \quad (4)$$

$$\hat{R}_k = \frac{1}{\#X \hat{c}_k} \sum_{x \in X} \pi_k(x) (x - \hat{\mu}_k)(x - \hat{\mu}_k)^T, \quad (5)$$

5 where  $\#X$  denotes the cardinality of set  $X$ . All data  
6 points contribute to estimate the means and covari-  
7 ances associated to all mixture modes but with differ-  
8 ent weights. Both steps are recursively computed until  
9 convergence is achieved. The number of modes,  $M$ , is  
10 either assumed a priori known or estimated from the  
11 data by a suitable method, e.g., minimum description  
12 length (MDL) [10]. The EM algorithm allows one to  
13 split the manifold into  $M$  disjoint regions,  $\mathcal{M}_i$ , accord-  
14 ing to a set of discriminant functions defined by the  
15 squared Mahalanobis distance

$$d(x, \mu_i)^2 = (x - \mu_i)^T R_i^{-1} (x - \mu_i). \quad (6)$$

17 For the sake of describing the manifold one should  
18 define local coordinates in each region. This can be  
19 done by applying principal component analysis (PCA)  
20 [9] to each region, using the second order statistics  
21  $\mu_i, R_i$ . The PCA defines an orthogonal basis in each  
22 region associated with the eigenvectors of the covari-  
23 ance matrix. Each point  $x \in \mathcal{M}_i$  is given by

$$x = \mu_i + V_i x_i, \quad (7)$$

23 where  $\mu_i$  is the mean of the  $i$ th region,  $V_i$  is a  
24  $n \times n$  matrix whose columns are the eigenvectors of  
25 the covariance matrix and

$$x_i = V_i^T (x - \mu_i) \quad (8)$$

are the local coordinates of  $x$  on  $\mathcal{M}_i$ .

If the smallest eigenvalues of the covariance ma-  
trix are close to zero an approximation may be con-  
sidered in which their corresponding eigenvectors are  
removed from  $V_i$ . In this case,  $V_i$  becomes a  $n \times m$   
matrix and equation  $\hat{x} = \mu_i + V_i x_i$  defines the orthogo-  
nal projection of  $x$  on the hyperplane spanned by the  
columns of  $V_i$ .

The hyperplane dimension (number of basis func-  
tions) depends on the eigenvalues of the covariance  
matrix. To keep the mean square error small, only the  
axes corresponding to small eigenvalues can be dis-  
carded. The mean square error,  $E^2$ , is given by

$$E^2 = \sum_{i=m+1}^n \lambda_i. \quad (9)$$

Fig. 4a shows the original data points on a parabolic  
surface (the surface is assumed to be unknown). Us-  
ing the EM method and PCA, this set is decomposed  
in disjoint classes, each one being approximated by a  
local hyperplane (Fig. 4b). The data points are pro-  
jected into the closest local hyperplane, their local co-  
ordinates being computed according to (8) (see Fig.  
4c). The data points are projected into the local hyper-  
plane and their local coordinates are computed. The  
data inside each region is approximated by a set of  
prototypes (centroids) obtained by the  $k$ -means al-  
gorithm [9]. The set of centroids associated to all the  
regions is denoted by  $U$ . The DMA algorithm adopts  
a discrete representation of the manifold, each mani-  
fold region being approximated by a set of prototypes  
 $U_i = \{u_{i1}, \dots, u_{in_i}\}$  expressed in local coordinates.

### 3.2. Motion and sensor model learning

A set of local Markov models is used to describe  
state trajectories inside the manifold regions. These  
local models are integrated in a global Markov model  
by considering trajectory transitions across the region  
borders. In this framework, trajectories are sequences  
of points on the manifold, corresponding to centroids  
on the hyperplanes.

Let  $x = (x(1), \dots, x(N)), x(t) \in M$ , be a trajectory  
on the manifold and  $u = (u(1), \dots, u(N)), u(t) \in U$  a  
sequence of centroids obtained by projecting each  
manifold point,  $x(t)$ , onto the closest hyperplane  
and approximating the projected point by the closest  
prototype (Fig. 5).

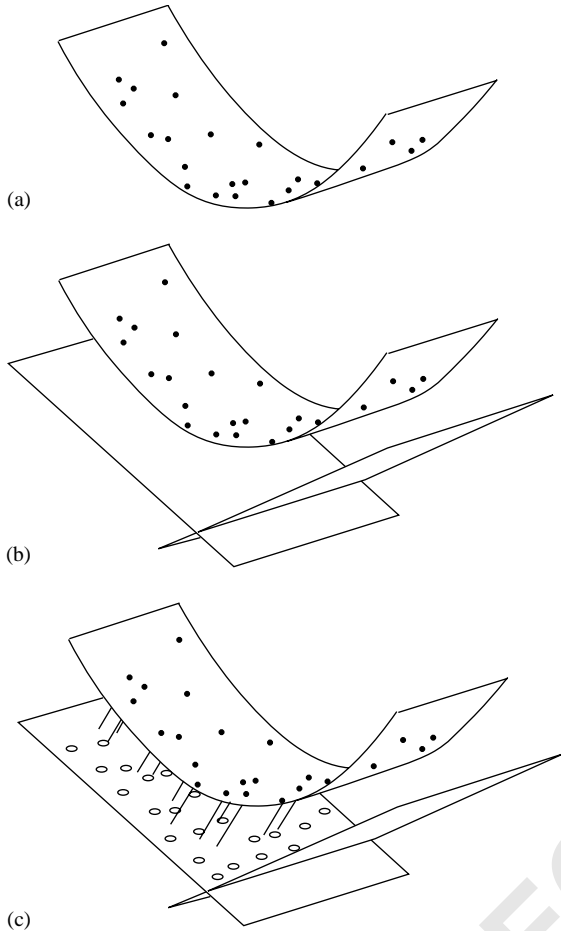


Fig. 4. Manifold learning: (a) original data points; (b) approximation of the manifold by local hyperplanes using EM (shifted downwards); (c) representation of projected data by centroids on the hyperplane.

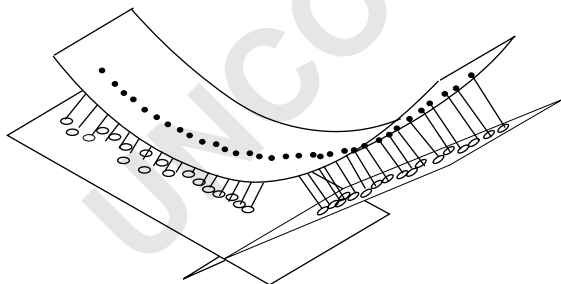


Fig. 5. Motion model: state trajectory and orthogonal projection and approximation by the nearest centroids.

It will be assumed that  $u$  is a random process which satisfies the Markov property of first order ( $P$  stands for probability)

$$P(u(t)/u(t-1), \dots, u(1)) = P(u(t)/u(t-1)). \quad (10)$$

The  $u$  trajectory inside a region  $M_i$  takes values in  $U_i$  and is described by a local Markov chain with transition matrix  $A^{ii} = (a_{kl}^{ii})$ ,

$$a_{kl}^{ii} = P(u(t) = u_{ik}/u(t-1) = u_{il}). \quad (11)$$

The  $u$  sequence is denoted as the *discrete state sequence*. Repeating this procedure for all manifold regions leads to  $M$  local Markov chains which define the motion models inside the regions.

To deal with transitions between two regions  $M_i, M_j, i \neq j$ , cross transition matrices  $A^{ij} = (a_{kl}^{ij})$ ,

$$a_{kl}^{ij} = P(x(t) = u_{ik}/x(t-1) = u_{jl}) \quad (12)$$

are considered. The cross-transition matrices link all the local Markov models into a global model (Fig. 3) with transition matrix defined by

$$A = \begin{bmatrix} A^{11} & A^{12} & \dots & A^{1M} \\ \vdots & \vdots & \vdots & \vdots \\ A^{M1} & A^{M2} & \dots & A^{MM} \end{bmatrix}. \quad (13)$$

In general  $A$  is a stochastic matrix whose entries may all be nonnegative. However,  $A$  is actually a sparse matrix in many situations (e.g., when a motion is being considered as in the example of Fig. 3) since most of the cross transitions have zero probability. This property stresses the physical meaning of the local Markov chains which describe the motion inside the manifold regions. Although the motivation for building matrix  $A$  stems from time and state discretization of a diffusion model which represents the motion considered, it is remarked that the methods described in this paper apply to general Markov chains. It should also be mentioned that the complexity of matrix  $A$  should be low enough so as to allow its estimation from available data.

In this paper, matrix  $A$  is estimated by computing the relative frequencies of all possible state transitions, a procedure justified by the strong law of large numbers. This amounts to assume available a sufficiently rich set of trajectories covering the whole manifold. The estimates converge almost surely to the true value as the number of points tends to infinity. To estimate the manifold sequence a sensor model is required. Let

1  $y = (y(1), \dots, y(N))$  be an observation sequence. It  
 2 will be assumed that  $y(t)$  is an instantaneous measure-  
 3 ment of  $u(t)$  being characterized by the probability  
 4 function  $p(y(t)/u(t))$  which has to be estimated from  
 5 the data.

6 The motion model  $P(u(t)/u(t-1))$  and the sensor  
 7 model  $p(y(t)/u(t))$  define a hidden Markov model.

### 3.3. Trajectory retrieval

9 It is not usually possible to estimate  $u(t)$  from a  
 10 single observation  $y(t)$  since in this case it is not possi-  
 11 ble to exploit the dynamical properties of the state  
 12 trajectory  $u$ . The estimation of the manifold trajec-  
 13 tory  $x$  is performed in two steps: (i) estimation of  
 14  $u$  and (ii) projection of  $u$  onto the manifold. Projec-  
 15 tion is performed by (7). Therefore, only the first step  
 16 has to be addressed. This is a well-known problem in  
 17 HMM theory which can be solved either by using the  
 18 forward-backward algorithm or the Viterbi algorithm  
 19 [8]. The first is used when an on-line estimate of the  
 20 state variable is required, relying only on current and  
 21 past observations while the Viterbi algorithm provides  
 22 the optimal state trajectory assuming that all observa-  
 23 tions (including future observations) are known.

## 4. Experimental results

25 Hereafter, the DMA algorithm is evaluated with  
 26 both synthetic and real data. Three examples will be  
 27 described to illustrate the concepts presented in the  
 28 paper.

### 4.1. Example 1

31 Fig. 6 shows the retrieval of trajectories on a sphere  
 32 from incomplete and noisy measurements. In this  
 33 example, the motion is a known Markov chain on  
 34 the sphere and the observations are obtained by  
 35  $y = [1 \ -11]x + v$  where  $v$  is white Gaussian noise,  
 36 i.e.,  $y$  is a linear combination (projection onto a line)  
 37 of the Cartesian coordinates of the point  $x$  on the  
 38 sphere, corrupted by additive noise.

39 Since the observation model is noninvertible, the  
 40 state cannot be recovered from a single measurement.  
 41 Each observation defines a plane which intersects the  
 42 sphere at an infinite number of points, located along

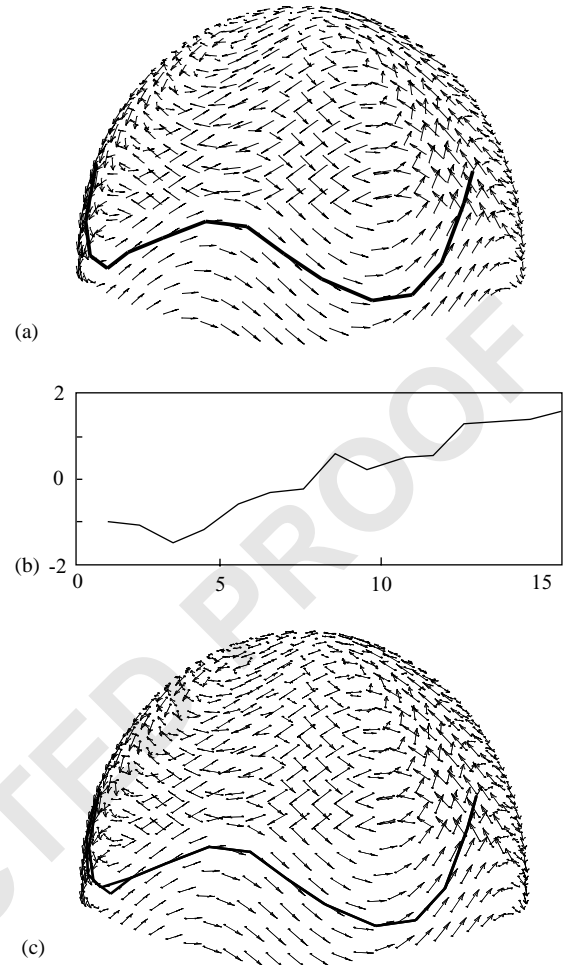


Fig. 6. Trajectory estimation on manifolds: (a) true trajectory  
 (b) noisy observations (c) retrieved trajectory (arrows define the  
 motion field; the starting point of each arrow corresponds to a  
 centroid).

a circle. To recover the  $x$  trajectory it is necessary to  
 use information about the motion dynamics and the  
 manifold geometry. 43

In this example, a velocity field was defined on the  
 sphere. The velocity field is used to compute the al-  
 lowed transitions among the centroids. Fig. 6a shows  
 the centroids and the velocity field defined on the  
 sphere surface. A state trajectory generated by the  
 HMM is also displayed. Figs. 6b and c show the ob-  
 servation sequence associated to the trajectory and the  
 trajectory estimate obtained by the DMA algorithm. 45  
 47  
 49  
 51

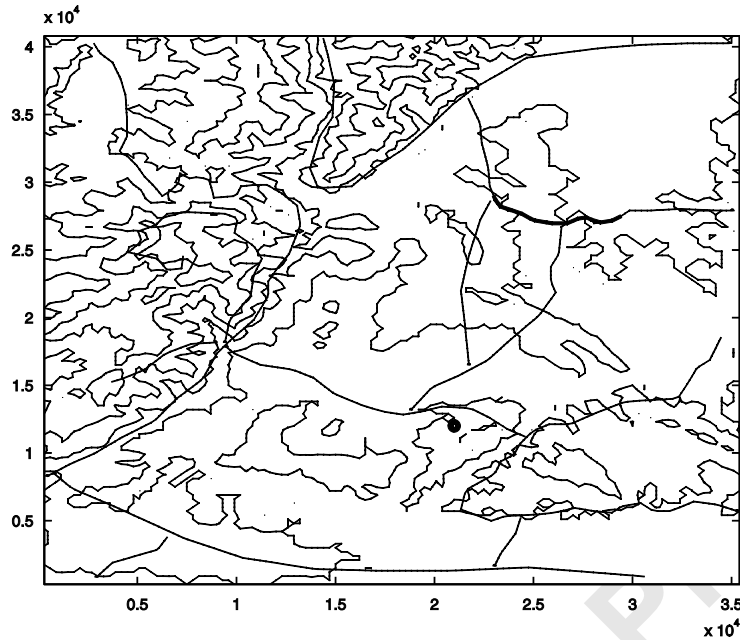


Fig. 7. Digital elevation map and road network (the car trajectory is displayed in bold and the receiver is identified by a circle).

1 A perfect reconstruction was achieved (the right cen-  
 2 troids were selected), except at the first two instants  
 3 of time. We stress that this problem cannot be solved  
 4 by standard estimation methods which do not restrict  
 5 the state to lie on the manifold.

#### 4.2. Example 2

7 The second example considers the problem of  
 8 estimating the position of a vehicle moving along  
 9 trajectories in a three-dimensional manifold given by  
 10 the roads in a map. It is assumed that only the dis-  
 11 tance to the receiver is known. Since the road map  
 12 is assumed to be known, the first step of the DMA  
 13 is not actually used in the example. Fig. 7 shows the  
 14 manifold contour map together with the trajectory to be  
 15 detected (bold line). The units in both scales are [m].  
 16 From the point located with a dot, radar observations  
 17 are made according to the model

$$y_t = \cos(\omega d_t) + w_t, \quad (14)$$

18 where  $y_t$  is the signal measured at time  $t$ ,  $\omega=0.02$ ,  $d_t$   
 19 is the distance to the observation point and  $w_t$  is white  
 noise,  $w_t \tilde{N}(0, \sigma^2 = 0.05)$ .

Fig. 8 shows the estimated path of the vehicle  
 yielded by the DMA algorithm.

21

#### 4.3. Example 3

22 The third example illustrates the performance of the  
 23 DMA algorithm in a tracking experiment. Fig. 9 shows  
 24 the results of the DMA algorithm in the estimation of  
 25 a slot-race car trajectory on a video sequence of 593  
 26 images obtained at 12 fps. For this sake a background  
 27 image is subtracted from each new frame. The image  
 28 difference is then compared to a threshold and the  
 29 number of active pixels in the vicinity of each centroid  
 30 is computed. Let  $y_t$  denote the  $t$ th image. It is assumed  
 31 that

$$p(y_t/u_k) = \begin{cases} cn_k, & 0 \leq n_k \leq L^2, \\ 0, & \text{otherwise,} \end{cases} \quad (15)$$

32 where  $n_k$  is the number of active pixels in a  $L \times L$   
 33 square region centered at  $u_k$ .

34 Figs. 9a and d show four consecutive images ex-  
 35 tracted from this sequence. Due to motion, the car is

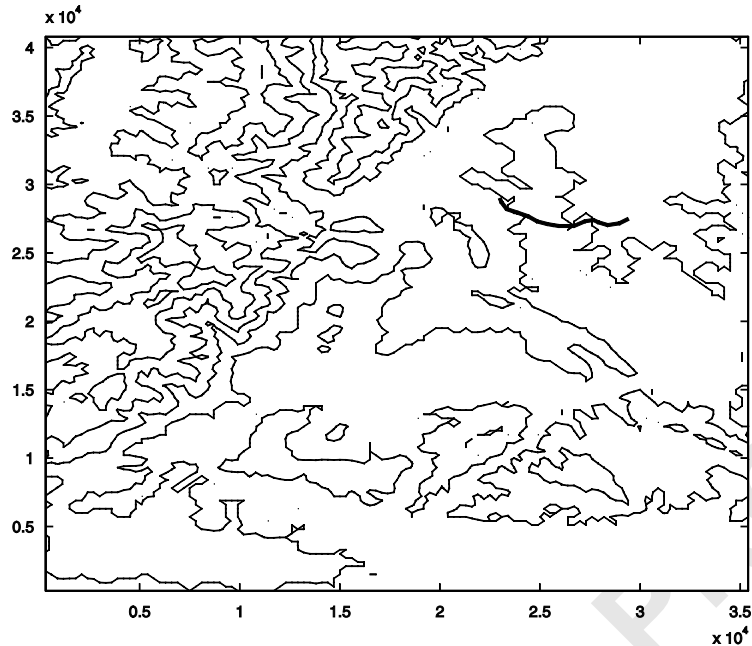


Fig. 8. Estimated trajectory.

not always easy to detect. This difficulty will be overcome by using the manifold and the motion restrictions. Fig. 9e shows the car trajectories used to train the model as well as the local frames computed by the DMA algorithm. The estimation of the car position in the training phase was performed manually. However, trajectory retrieval experiments use automatic image processing techniques.

The HMM parameters (transition matrix and sensor model) were estimated from the training set by the strong law of large numbers. Fig. 9f shows the tracking results obtained with the DMA algorithm for a sequence of 7 consecutive images. Since all the frames are known, the Viterbi algorithm was used for trajectory retrieval. The true locations are also displayed for comparison. Good results were achieved even when the car is occluded by the bridge.

None of the problems described in this section can be solved without the geometric information learned from the training set in an early stage of the procedure and defining the manifold on which the state vector is assumed to exist. This information is embodied in the centroid positions.

## 5. Conclusion

This paper exploits geometric restrictions for solving estimation problems in dynamic scene analysis. Although the primary motivation stems from image processing problems, the methods described may also be used in relation to control systems where parameters slowly move on a manifold due to changes in plant operating condition. An algorithm is proposed to estimate unknown state trajectories in manifolds. This algorithm denoted as discrete manifold analysis (DMA) allows to use the available information about the manifold geometry, as well as the motion dynamics and the sensor model. The manifold is split into disjoint regions, each of them being approximated by a hyperplane. This allows to reduce the dimensionality of the unknown data and to simplify the description and estimation of the state trajectories. A set of local hidden Markov models (HMM) is used to represent the state trajectories inside each region and the observation sequence. To allow transitions between different regions, a global HMM is defined by completing the local descriptions, valid inside the manifold regions, with transition models. The state trajectory is



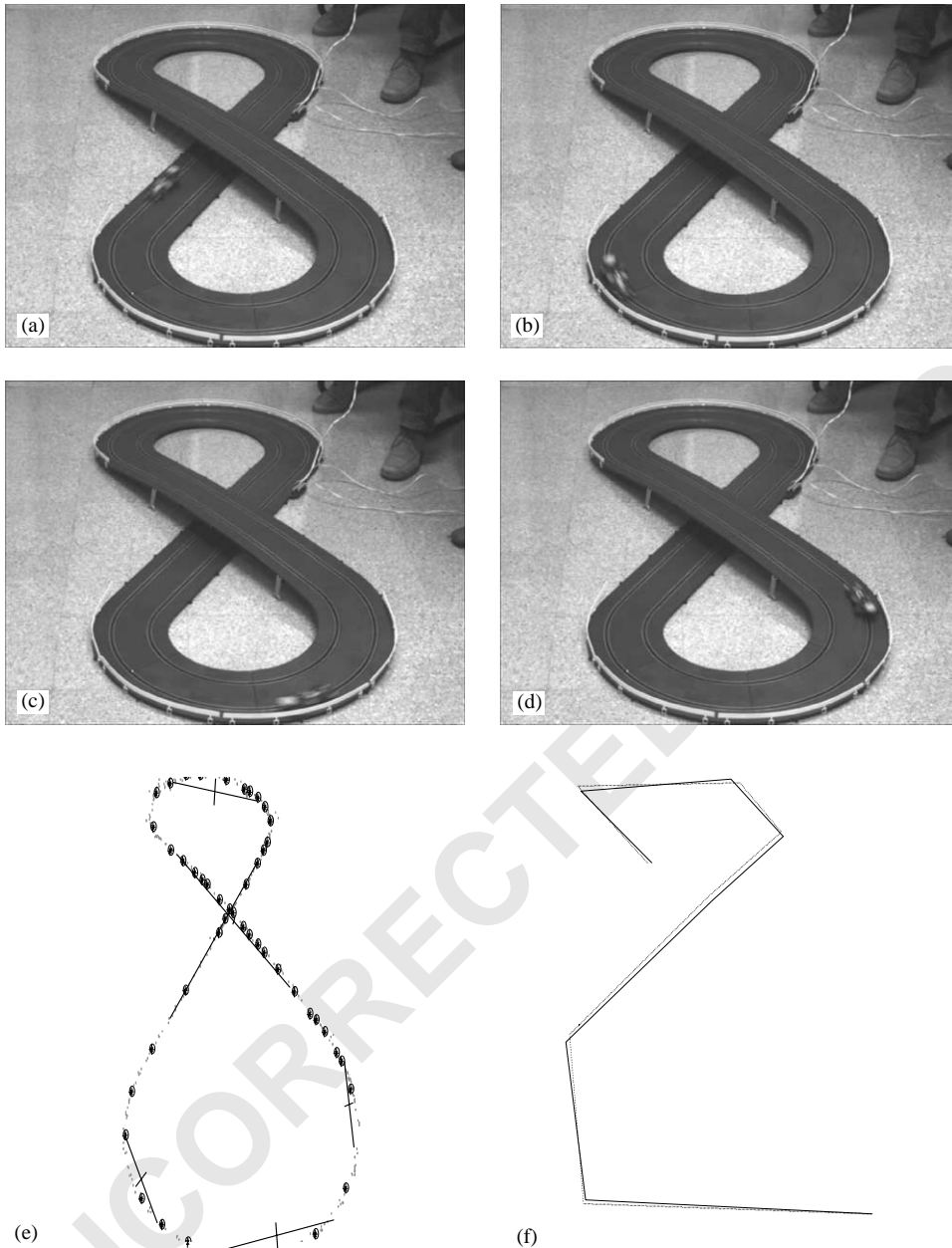


Fig. 9. Results of DMA algorithm: (a–d) input images; (e) training data, local frames and centroids; (f) true and retrieved trajectories (black dots represent centroids, single dots represent training observations, straight lines represent principal axis (e) and car trajectories (f)).

1 recursively estimated by dynamic programming. The  
 2 experimental results presented in the paper show the  
 3 ability of the DMA algorithm to estimate state trajec-  
 4 tories on manifolds, exploiting the information on the

5 manifold geometry as well as the motion and sensor  
 6 information.

7 To sum up, the advantage of the proposed approach  
 8 comes from: (1) the use of hyperplanes for manifold

1 approximation; (2) discretization, which allows for the  
possibility of using the nonlinear HMM description.

### Acknowledgements

The authors thank the anonymous reviewers for the valuable comments which helped to improve the paper.

### References

- 5 [1] J. Biemond, R. Lagendijk, R. Mersereau, Iterative methods  
for image deblurring, Proc. IEEE (1990).
- 7 [2] A.F. Bobick, A.D. Wilson, A state-based approach to the  
representation and recognition of gesture, Trans. Pattern Anal.  
9 Mach. Intell. (December 1997) 1325–1337.
- 11 [3] C. Bregler, S. Omohundro, Nonlinear manifold learning for  
visual speech recognition, Internat. Conf. Comput. Vision  
(1995) 494–499.
- 13 [4] J. Clark, An introduction to stochastic differential equations  
on manifolds, in: Geometric Methods on Systems Theory,  
15 Reidel, Dordrecht, 1973.
- [5] R. Marino, P. Tomei, Nonlinear Control Design,  
Prentice-Hall, Englewood Cliffs, NJ, 1995. 17
- [6] H. Murase, S. Nayar, Visual learning and recognition of  
3-D objects from appearance, Internat. J. Comput. Vision 14 19  
(1995) 5–24.
- [7] W. Press, S. Teukolsky, W. Vetterling, B. Flannery,  
Numerical Recipes in C, Cambridge University Press,  
Cambridge, 1994. 21
- [8] L. Rabiner, A tutorial on hidden Markov models and selected  
applications in speech recognition, Proc. IEEE. (1989) 257– 23  
286. 25
- [9] B. Ripley, Pattern Recognition and Neural Networks,  
Cambridge University Press, Cambridge, 1996. 27
- [10] J. Rissanen, Universal coding, information, prediction and  
estimation, IEEE Trans. Inform. Theory (1984). 29
- [11] R. Sara, R. Bajcsy, Fish-scales: representing fuzzy manifolds,  
Internat. Conf. Comput. Vision (1998). 31
- [12] R. Szeliski, Bayesian Modeling of Uncertainty in Low-Level  
Vision, Kluwer Academic Publishers, Dordrecht, 1989. 33
- [13] N. Winters, S. Santos-Victor, Omni-directional visual  
navigation, Internat. Symp. Intell. Robotic Systems, 1999. 35